ADP-Ribosylation of α_{i3}C20 by the S1 Subunit and Deletion Peptides of S1 of Pertussis Toxin†

Viviane Finck-Barbançon and Joseph T. Barbieri*

Department of Microbiology, Medical College of Wisconsin, 8701 Watertown Plank Road, Milwaukee, Wisconsin 53226

Received March 8, 1994; Revised Manuscript Received November 9, 1994®

ABSTRACT: Recombinant S1 subunit of PT (rS1) and two carboxyl-terminal deletion peptides, C180 and C204, which comprise the amino-terminal 180 and 204 amino acids of S1, respectively, were analyzed for the ability to ADP-ribosylate α_{i3}C20, a synthetic peptide composed of the 20 carboxyl-terminal amino acids of the α subunit of the heterotrimeric G protein G_{i3}. Under linear velocity conditions, C180 ADP-ribosylated α_{i3}C20 at a 3-fold higher rate than either C204 or rS1. At variable NAD, rS1, C204, and C180 ADP-ribosylated α_{i3}C20 with similar initial velocities which followed Michaelis−Menten kinetics. In contrast, at variable α_{i3}C20, rS1, C204, and C180 ADP-ribosylated α_{i3}C20 with different initial velocities. At variable α_{i3}C20, C204- and rS1-catalyzed ADP-ribosylation followed Michaelis−Menten kinetics, while the velocity curve generated by C180 diverged from Michaelis−Menten kinetics. The rates of initial velocity of C180 did not fit the Lineweaver−Burk equation, but could be transformed into the Hill equation which yielded a Hill coefficient of 2. This predicted that C180 possessed cooperativity between the two substrate binding sites. Other experiments showed that C180 ADP-ribosylated α_{i3}C20 at 60% of the rate for the ADP-ribosylation of G_t. These data showed that the entire catalytic mechanism for ADP-ribosylation resides within the first 180 amino acids of S1 and that the carboxyl-terminal 55 residues of S1 allow the ADP-ribosylation of α_{i3}C20 to proceed via Michaelis−Menten kinetics. These data along with earlier studies (Krueger & Barbieri, 1993) were also consistent with the presence of two G_t protein binding sites within S1. One G protein binding site was located within the amino-terminal 180 residues of S1 and interacted with a region of $G_{t\alpha}$ defined by α_{i3}C20. The second G protein binding site was defined by residues 195−204 of S1 and was located within $G_{t\alpha}$ but outside the α_{i3}C20 binding site. This second interaction provides a greater k_{cat} and lower K_{mG_t} for the ADP-ribosylation of the heterotrimeric G_t by S1.

Pertussis toxin (PT, M_r 105 890) is a major virulence determinant of *Bordetella pertussis*, the causative agent of whooping cough (Weiss & Falkow, 1984). PT is a member of the family of bacterial ADP-ribosylating enzymes which catalyze the transfer of the ADP-ribose moiety of NAD to specific eucaryotic target proteins (Katada *et al.*, 1982; Ui, 1990). PT is composed of 6 proteins, designated S1 through S5, which are noncovalently associated in a 1:1:1:2:1 ratio, respectively (Tamura *et al.*, 1982). PT follows the "A:B" model for exotoxin structure−function (Tamura *et al.*, 1982; Ui, 1990), where the "A" domain (S1) contains the ADP-ribosyltransferase activity, and the "B" domain (S2 through S5) binds to the cell surface receptors to allow passage of S1 across the cell membrane. S1 catalyzes the ADP-ribosylation of a conserved cysteine residue located 4 amino acids from the carboxyl terminus of the α subunits of a subset of heterotrimeric GTP-binding proteins, G_i, G_o, and G_t (Van Dop *et al.*, 1984; West *et al.*, 1985; Hsia *et al.*, 1985; Birnbaumer *et al.*, 1990), which uncouples signal transduction between the G protein and its G protein coupled receptor (Ui, 1990; Conklin & Bourne, 1993).

The operon encoding the PT subunits has been cloned and sequenced (Locht *et al.*,1986; Nicosia *et al.*, 1986), and the genes encoding the individual subunits of PT have been expressed in *Escherichia coli* (Barbieri *et al.*, 1987; Burnett *et al.*, 1988; Locht *et al.*, 1987; Nicosia *et al.*, 1987). Biochemical studies showed that recombinant S1 (rS1) possessed similar kinetic properties as S1 (235 amino acids) purified from pertussis toxin (Barbieri *et al.*, 1990). Analysis of deletion peptides of S1 identified regions of S1 that were responsible for catalysis. The C180 peptide which comprised residues 1−180 catalyzed the NAD glycohydrolase reaction at the same rate as S1, but ADP-ribosylated the heterotrimeric G protein, G_t, at 1% of the rate of S1 (Cortina & Barbieri, 1991). Kinetic studies showed that C180 possessed a higher K_{mGt} and a lower k_{cat} than S1 (Cortina *et al.*, 1991). These studies also showed that S1 ADP-ribosylated G_t at a 17-fold higher rate than the isolated $G_{t\alpha}$ subunit, while C180 ADP-ribosylated G_t at a rate that was less than 2-fold higher than the isolated $G_{t\alpha}$ subunit. These data indicated that the high affinity of rS1 for heterotrimeric G_t was due, either directly or indirectly, to interactions of the carboxyl-terminal 55 amino acid residues of S1 with $G_{t\beta\gamma}$. Analysis of deletion peptides of S1 showed that residues between 195 and 204 were responsible for the high affinity binding of S1 to G_t (Cortina *et al.*, 1991; Krueger & Barbieri, 1994).

Moss and co-workers (Watkins *et al.*, 1985) reported that tryptic peptides of $G_{t\alpha}$ were not ADP-ribosylated by PT, which suggested that PT recognized the conformation of $G_{t\alpha}$. Recently, Birnbaumer and co-workers (Graf *et al.*, 1992) showed that peptides comprising the 10−20 carboxyl-

† This research was supported by Public Health Grants AI-30162 and AI-01087 (J.T.B.) from the National Institutes of Health. V.F.-B. is supported by a fellowship from the International Human Frontier Science Program.

* Phone (414) 456-8412; fax (414) 266-8522.

® Abstract published in *Advance ACS Abstracts,* December 15, 1994.

0006-2960/95/0434-1070$09.00/0

terminal residues of the α subunit of PT-sensitive G proteins, including G_i, were substrates for ADP-ribosylation by PT. In the present study, we measure the ability of S1 and two deletion peptides to ADP-ribosylate α_{i3}C20, a synthetic peptide composed of the 20 carboxyl-terminal amino acids of the α subunit of the heterotrimeric G protein G_{i3}. These studies allowed the localization of several functions within the carboxyl-terminal 55 amino acids of S1.

MATERIALS AND METHODS

Materials

Construction of ptacS1c, ptacC180, and ptdlC204 has been described previously (Barbieri *et al.*, 1989; Krueger & Barbieri, 1994). [*adenylate phosphate*-^{32}P]NAD was purchased from Du Pont-New England Nuclear. Protein molecular mass markers were purchased from Pharmacia-LKB Biotechnology Inc. Analysis of kinetic data was performed with the software "Enzfitter" (Elsevier-Biosoft, Cambridge, U.K.). Transducin (G_t) was purified from bovine retina (J. A. Lawson Co., Lincoln, NE) as previously described (Cortina & Barbieri, 1991).

Methods

Synthesis of α_{i3}C20 Peptide. The 20 amino acid peptide NH_2-VFDAVTDVIIKNNLKECGLY-COOH (termed α_{i3}-C20) was synthesized at the Shared Protein-Nucleic Acid Facility at the Medical College of Wisconsin. The composition of α_{i3}C20 was confirmed by amino acid and mass spectroscopic analysis. HPLC analysis showed the purity of the peptide to be 72%. The α_{i3}C20 peptide was soluble in 0.1 N NH_4OH and stored at −20 °C.

Purification of rS1, C180, and C204. (A) rS1. Purification of rS1 from *E. coli* has been described (Xu *et al.*, 1994) with the indicated modifications. Overnight cultures of *E. coli* (ptacS1c) were diluted 1/50 into 2.4 L of 2 × L-Broth supplemented with 100 μg of ampicillin/mL and 0.5 mM $ZnSO_4$ and incubated for 6 h at 30 °C at 250 rpm. Cells were concentrated, washed, suspended in 20 mL of 25 mM Tris-HCl (pH 7.6), and broken by two passes through a French press. French-pressed cells were centrifuged (3000*g*) for 5 min to pellet unbroken cells and then centrifuged at 45000*g* for 35 min to pellet insoluble material. This insoluble material was suspended in 20 mL of 25 mM Tris-HCl (pH 7.6), 100 mM NaCl, and 2% Triton X-100 and centrifuged at 45000*g* for 35 min. This insoluble material was suspended in 25 mM Tris-HCl (pH 7.6) and 1 M NaCl and centrifuged for 30 min at 45000*g*. The insoluble material was then suspended in 25 mM Tris (pH 7.6) containing 8 M urea overnight at 4 °C and centrifuged at 163000*g* for 2 h; the soluble fraction was chromatographed over a S-200 HR Sephacryl in 25 mM Tris-HCl (pH 7.6) containing 4 M urea. Column fractions containing rS1 were pooled and concentrated by ammonium sulfate precipitation (50% final concentration). Prior to analysis, an aliquot of rS1, stored as an ammonium sulfate precipitate, was pelleted by centrifugation and resuspended in 25 mM Tris-HCl (pH 7.6) containing 1 M urea.

(B) C180. Purification of the C180 peptide was as described previously (Barbieri *et al.*, 1989). Briefly, 6 L of *E. coli* (ptacC180) was cultured for 6−8 h in the presence of 100 μg of ampicillin/mL and 0.5 mM $ZnSO_4$. The C180 peptide was purified from a periplasmic fraction via conventional chromatography and stored as an ammonium sulfate precipitate.

(C) C204. Purification of C204 peptide has been described (Krueger & Barbieri, 1994). Briefly, 2.4 L of *E. coli* (ptdlC204) was grown for 6 h (OD_{600} <1) in the presence of 100 μg of ampicillin/mL and 0.5 mM $ZnSO_4$ at 30 °C and 250 rpm. C204 was purified from a periplasmic fraction by conventional chromatography and stored as an ammonium sulfate precipitate. Purified rS1, C180, and C204 peptides were subjected to SDS−PAGE in the presence of β-mercaptoethanol and stained for protein with Coomassie Blue.

ADP-Ribosylation of α_{i3}C20 Peptide or G_t. Linear velocity activities of rS1, C180, or C204 were determined in reaction mixtures containing: 0.1 M Tris-HCl (pH 7.6), 20 mM DTT, 0.4 mg of egg albumin/mL, [*adenylate phosphate*-^{32}P]NAD (specific activity was adjusted by addition of cold NAD), the indicated concentration of α_{i3}C20 or G_t, and either C180, C204, or rS1 which was added to start the reaction. α_{i3}C20 was incubated with 50 mM DTT on ice for 10 min prior to the assay. After 30, 60, 90, or 120 min of incubation at 4 °C, 20 μL aliquots were removed and spotted onto trichloroacetic acid saturated Whatman 3MM chromatography paper. Papers were washed three times for 20 min with 100 mL of 7.5% trichloroacetic acid, soaked once in methanol, dried, and subjected to scintillation counting. The amount of α_{i3}C20 or NAD utilized was less than 15%. Initial velocities [mol of α_{i3}C20 peptide ADP-ribosylated/(min·mol of enzyme)] were calculated from the linear region of the plot of ^{32}P incorporated into the α_{i3}C20 peptide *versus* time. The amount of α_{i3}C20 peptide or rS1 and its deletion peptides was determined as described in Quantitation of Peptides (see below) and used to normalize the velocities.

Experiments that measured the ADP-ribosylation of α_{i3}-C20 by C180 as a function of temperature were performed as described above with assays being performed in parallel at 4, 11, 22, 30, 37, or 42 °C at either 1, 3, or 10 μM NAD and 3 μM α_{i3}C20. Experiments that measured the ADP-ribosylation of α_{i3}C20 by C180 as a function of NaCl were performed as described above in the presence of 0−1.0 M NaCl at 10 μM NAD (specific activity was adjusted to 4 × 10^2 cpm/pmol) and 3 μM α_{i3}C20 at 4 °C for 60 min. Experiments that measured the rate of ADP-ribosylation of α_{i3}C20 by rS1, C204, and C180 were performed as described above at 10 μM NAD (specific activity was adjusted to 1.5 × 10^3 cpm/pmol) and 3 μM α_{i3}C20. C180, C204, and rS1 were incubated in 50 mM Tris-HCl (pH 7.6) containing 0.1 mg of egg albumin/mL and 20 mM DTT for 20 min at room temperature prior to the start of the assay which was performed at 4 °C.

Determination of Kinetic Constants of C204, C180, and rS1 for NAD and α_{i3}C20. (A) Variable α_{i3}C20. Reaction mixtures contained in 25 μL: 0.1 M Tris-HCl (pH 7.6), 20 mM DTT, 0.4 mg of egg albumin/mL, 10 μM [*adenylate phosphate*-^{32}P]NAD (specific activity 2 × 10^3 cpm/pmol), varying concentrations of α_{i3}C20 (between 4 and 100 μM), and an aliquot of rS1, C204, or C180. α_{i3}C20 was prepared by a 10 min incubation on ice in 0.1 N NH_4OH containing 50 mM DTT followed by serial dilution in 0.1 N NH_4OH prior to assay. After incubation at 4 °C for 30 min, incorporation of ^{32}P into trichloroacetic acid precipitable material was determined as described above. Utilization of NAD or α_{i3}C20 peptide was <5%. Data were transformed

Table 1: Effect of Temperature on C180 ADP-ribosylation of α_{i3}C20 as Target

NAD (μM)	velocity[a] [mol/(min·mol)] at T (°C): 4	11	22	30	37	42	37 → 4[b]	37 → 37[c]
1	0.08 ± 0.01	ND[d]	0.04 ± 0.01	ND[d]	0.01 ± 0.01	ND[d]	ND[d]	ND[d]
3	0.08 ± 0.01	ND[d]	0.05 ± 0.01	ND[d]	0.02 ± 0.01	ND[d]	ND[d]	ND[d]
10[e]	0.19 ± 0.02	0.20 ± 0.01	0.23 ± 0.01	0.14 ± 0.01	0.07 ± 0.01	0.031 ± 0.01	0.12 ± 0.01	0.06 ± 0.01

[a] Incubations were as described in Materials and Methods, and rates are expressed as moles of ADP-ribose incorporated into α_{i3}C20 peptide per minute per mole of C180. [b] After incubation of α_{i3}C20 at 37 °C for 30 min prior to its utilization, assay was then performed at 4 °C as described in Materials and Methods. [c] After incubation of α_{i3}C20 at 37 °C for 30 min prior to its utilization, assay was performed at 37 °C. [d] Not determined. [e] Values are the average of at least two separate experiments performed in parallel at 4, 11, 22, 30, 37, and 42 °C.

into Lineweaver–Burk or Hill equations with the assistance of Enzfitter (Elsevier, U.K.).

(B) Variable NAD. Assays were performed as described above for variable α_{i3}C20 with the following modifications: the concentration of α_{i3}C20 peptide was 46 μM and NAD was varied between 0.3 and 10 μM. In these assays, <10% of the available NAD was utilized. Experiments were performed twice using the same enzyme preparations.

Quantitation of Peptides. (A) α_{i3}C20 or G_t. The concentration of α_{i3}C20 or G_t was calculated from a first-order rate projection of the maximum amount of ^{32}P incorporated after incubation of α_{i3}C20 or G_t with excess [*adenylate phosphate*-^{32}P]NAD and C180 or rS1, respectively.

(B) rS1, C204, and C180 Peptides. Peptides were quantitated as described previously (Cortina & Barbieri, 1991). Briefly, peptides that had been subjected to SDS–PAGE followed by Coomassie staining were quantitated by densitometry (AMBIS optical imaging system) *versus* a standardized preparation of C180 (Barbieri *et al.*, 1989). Peptide concentrations were adjusted for band intensities with respect to their length.

RESULTS AND DISCUSSION

Birnbaumer and co-workers (Graf *et al.*, 1992) reported that synthetic peptides corresponding to the 10–20 carboxyl-terminal residues of the α subunits of heterotrimeric G proteins, including G_{i3}, were substrates for ADP-ribosylation by PT. The affinity of PT for the α_{i3}C20 peptide was about 10-fold lower than that of either the heterotrimeric G_{i3} or the isolated $G_{\alpha i3}$ subunit, while the k_{cat} of PT for α_{i3}C20 was 15-fold lower than that of the heterotrimeric G_{i3}, but 10-fold higher than the $G_{\alpha i3}$ subunit.

One focus of PT research has been to determine specific amino acids that participate in the ADP-ribosyltransferase reaction with the goal of engineering noncatalytic forms of PT for vaccine development. One limitation to these studies has been the inability to purify the heterotrimeric G protein at concentrations sufficiently above their apparent K_ms to achieve zero-order kinetics. Since the α_{i3}C20 peptide was a target for ADP-ribosylation by PT and could be analyzed at concentrations beyond those required to achieve zero-order kinetics, α_{i3}C20 appeared to be a useful tool for the kinetic characterization of mutated derivatives of S1 that were deficient in the ADP-ribosylation reaction.

In an earlier study, we observed that wild-type C180 and a mutated peptide, C180H35Q, showed similar velocity curves in the ADP-ribosylation reaction at variable α_{i3}C20. The data could not be transformed to the Lineweaver–Burk equation, but did fit the Hill equation which showed that there was cooperative binding between NAD and α_{i3}C20 (Xu *et al.*, 1994). This observation initiated the present study to determine whether the cooperative binding observed during the ADP-ribosylation of α_{i3}C20 by C180 peptide was a unique property of C180 or a feature common to S1 or C204.

Temperature Effects on the Linear Velocity of C180-Catalyzed ADP-ribosylation of α_{i3}C20. In the initial description of the ADP-ribosylation of a synthetic peptide composed of the carboxyl-terminal 20 amino acids of the α subunit of heterotrimeric G protein G_{i3}, termed α_{i3}C20, reactions were performed at 4 °C (Graf *et al.*, 1992). To establish a standard assay for the ADP-ribosylation of α_{i3}-C20 by rS1, C204, and C180, the effect of temperature and ionic strength on the ADP-ribosylation of α_{i3}C20 by C180 peptide was measured. Rates of ADP-ribosylation of α_{i3}-C20 catalyzed by the C180 peptide did not increase proportionally with increasing temperature. At 10 μM NAD, the rates of ADP-ribosylation were similar between 4 and 22 °C (within 20%), while temperatures above 22 °C yielded lower rates of ADP-ribosylation (Table 1). At temperatures between 4 and 37 °C, the rates of ADP-ribosylation showed no detectable lag and were constant over a 2-h time course. This suggested that the lower rates of ADP-ribosylation at temperatures between 22 and 37 °C were not due to thermal inactivation of C180, since the thermal inactivation of C180 would have yielded a progressively lower rate of ADP-ribosylation over the time course. Two mechanisms could be responsible for the lower rate of ADP-ribosylation observed at higher temperatures: either α_{i3}C20 had undergone thermal unfolding or the -SH of the cysteine within α_{i3}C20 had undergone oxidation. To differentiate between these two possibilities, an experiment was performed to determine whether the inactivation at 37 °C was reversible by sequential treatment of α_{i3}C20 at 37 °C and then at 4 °C. The 2-fold increase in the initial velocity of the ADP-ribosylation of α_{i3}C20 indicated that at least a portion of the activity was reversible. This suggested that the lower rate observed at 37 °C was not due to irreversible oxidation of the -SH of the cysteine of α_{i3}C20, but more likely the result of a temperature-sensitive unfolding of α_{i3}C20. In contrast, at 42 °C, linear regression of the rate for ADP-ribosylation of α_{i3}C20 *versus* time did not intersect zero, suggesting that some C180 may have been inactivated during the time course. At 1 and 3 μM NAD, the rate of ADP-ribosylation of α_{i3}C20 was greater at 4 °C than either 37 or 22 °C. Subsequent velocity assays were performed in the presence of 10 μM NAD at 4 °C, which allowed our data to be compared to the results obtained by Birnbaumer and co-workers (Graf *et al.*, 1992).

NaCl Effect on the ADP-ribosylation of α_{i3}C20. To identify potential ionic or hydrophobic interactions between α_{i3}C20 and C180, the rate of ADP-ribosylation of α_{i3}C20 by C180 was measured as a function of NaCl concentration.

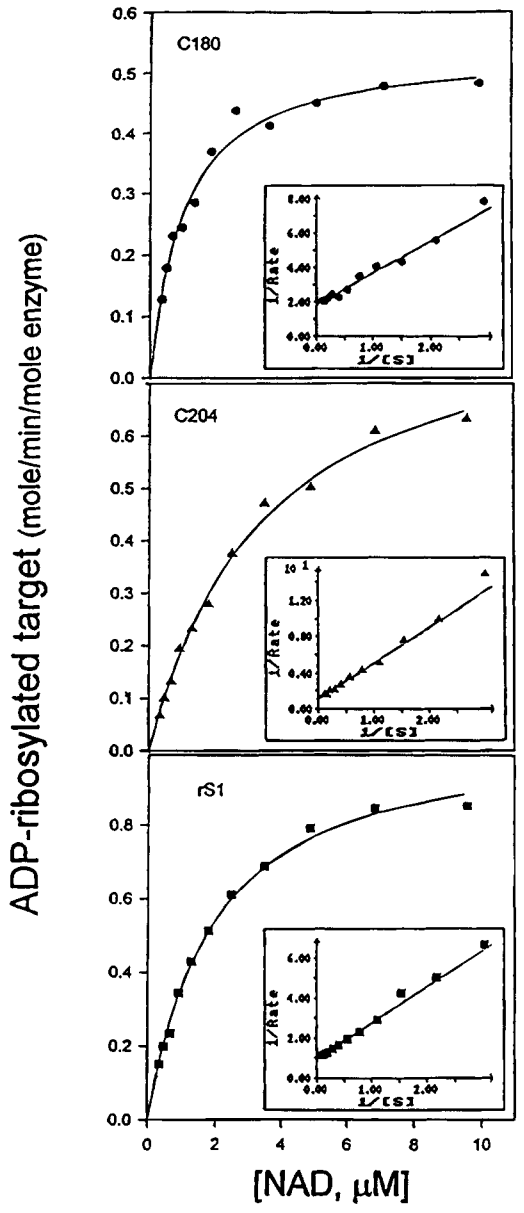

FIGURE 1: Velocity curves for the ADP-ribosylation of the α_{i3}C20 peptide by rS1, C204, and C180 as a function of NAD concentration. ADP-ribosylation was measured as the incorporation of radiolabel into α_{i3}C20 by rS1 (*lower panel*), C204 (*middle panel*), and C180 (*upper panel*) at varied concentrations of NAD and a constant concentration of α_{i3}C20 as described in Materials and Methods. The rate of the reaction is reported as mol of ADP-ribose incorporated into α_{i3}C20/(min·mol of enzyme). *Insets*: Lineweaver–Burk transformation of the data.

The rate of ADP-ribosylation of α_{i3}C20 by C180 varied less than 2-fold between 0 and 1 M NaCl (data not shown). This suggested that although both ionic or hydrophobic interactions may contribute to the ADP-ribosylation reaction, neither was dominant.

rS1-, C204-, and C180-Catalyzed ADP-ribosylation of α_{i3}C20. (A) Initial Velocities. Initial velocities for rS1-, C204-, and C180-catalyzed ADP-ribosylation of α_{i3}C20 were established where rates were linear with time (up to 120 min). At 10 μM NAD and 3 μM α_{i3}C20, rS1 and C204 ADP-ribosylated α_{i3}C20 at similar initial velocities of 0.1 mol/(min·mol of enzyme), while C180 ADP-ribosylated α_{i3}C20 at a 3-fold higher initial velocity of 0.3 mol/(min·mol of enzyme). Linear regression showed that neither S1, C204, nor C180 possessed a lag in the initiation of the ADP-ribosylation reaction, as has been observed for both PT and C204 in the ADP-ribosylation of G_t (Krueger & Barbieri, 1994).

Table 2: Kinetic Constants of C180-, C204-, and rS1-Catalyzed ADP-ribosylation of the α_{i3}C20 Peptide[a]

peptide	k_{cat} [mol/(min·mol)]	K_m or $S_{0.5}$ (μM)	k_{cat}/K_m or $k_{cat}/S_{0.5}$
	Variable NAD[b]		
C180	0.45 ± 0.08	0.9 ± 0.3	0.50
C204	0.85 ± 0.05	3.0 ± 0.6	0.3
rS1	1.0 ± 0.06	2.0 ± 0.1	0.50
	Variable α_{i3}C20[c]		
C180	2.0 ± 1	12.4 ± 0.3	0.16
C204	0.41 ± 0.1	6 ± 0.7	0.07
rS1	0.54 ± 0.1	11 ± 0.9	0.05

[a] Kinetic values, the average of two experiments, were determined following the transformation of linear velocities to the Lineweaver–Burk equation, except for the values shown for C180 with variable α_{i3}C20, which were determined following the transformation of the velocity curves to the Hill equation. [b] Assay conditions were 46 μM α_{i3}C20 at 4 °C, for 30 min. [c] Assay conditions were 10 μM NAD at 4 °C, for 30 min.

(B) Kinetic Constants for rS1, C204, and C180 in the ADP-Ribosylation of α_{i3}C20. (1) Variable NAD. At constant α_{i3}C20, rS1, C204, and C180 showed similar initial velocities in a dose-dependent response to NAD with saturating rates occurring by 6 μM NAD (Figure 1). Transformation of the initial velocities to the Lineweaver–Burk equation showed Michaelis–Menten kinetics with a K_{mNAD} of 1 μM for C180, 2 μM for rS1, and 3 μM for C204 (Table 2), about 6-fold lower than the K_{mNAD} reported for PT in the ADP-ribosylation of α_{i3}C20 (Graf *et al.*, 1992). The k_{cat} (min^{-1}) was 0.45 for C180, 0.85 for C204, and 1 for rS1, and the catalytic efficiencies (k_{cat}/K_{mNAD}) for the three peptides were within 2-fold.

(2) Variable α_{i3}C20. At constant NAD, although rS1, C204, and C180 achieved zero-order kinetics in a dose-dependent response to α_{i3}C20, their velocity curves were different (Figure 2). Transformation of the initial velocities of rS1-catalyzed ADP-ribosylation of α_{i3}C20 to a Lineweaver–Burk double reciprocal equation yielded Michaelis–Menten kinetics (Figure 2, *lower panel*) with a $K_{m\alpha_{i3}C20}$ of 11 μM and a k_{cat} (min^{-1}) of 0.54 (Table 2). This demonstrated that the two substrates, NAD and α_{i3}C20, bound independently to S1. Transformation of the initial velocities of C204-catalyzed ADP-ribosylation of α_{i3}C20 to the Lineweaver–Burk equation showed that although values at the lower concentrations of α_{i3}C20 diverged from the determined line (Figure 2, *middle panel*), the data could be plotted and yielded a $K_{m\alpha_{i3}C20}$ of 6 μM and a k_{cat} (min^{-1}) of 0.4. The initial velocities of C204-catalyzed ADP-ribosylation of α_{i3}-C20 could not be transformed into the Hill equation. In contrast, the initial velocities of C180-catalyzed ADP-ribosylation of α_{i3}C20 did not fit the Lineweaver–Burk equation (Figure 2, *upper panel inset*) and, therefore, did not follow Michaelis–Menten kinetics, which suggested that the NAD and α_{i3}C20 binding sites within C180 were not functioning independently. The initial velocities of C180-catalyzed ADP-ribosylation of α_{i3}C20 could be transformed into the Hill equation, which yielded a $S_{0.5\alpha_{i3}C20}$ of 12 μM and a k_{cat} (min^{-1}) of 2.0 for C180, with a Hill coefficient of 2, which indicated that there was cooperative binding

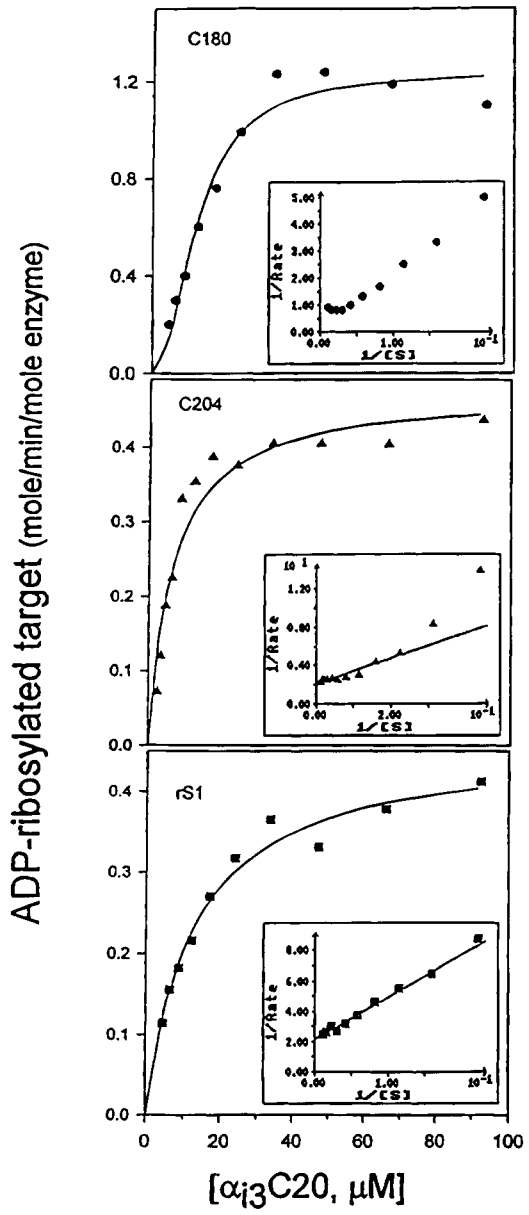

FIGURE 2: Velocity curves for the ADP-ribosylation of α_{i3}C20 peptide by rS1, C204, and C180 as a function of α_{i3}C20 peptide concentration. ADP-ribosylation was measured as the incorporation of radiolabel into α_{i3}C20 by rS1 (*lower panel*), C204 (*middle panel*), and C180 (*upper panel*) at varied concentrations of α_{i3}C20 and a constant concentration of NAD as described in Materials and Methods. The rate of the reaction is reported as mol of ADP-ribose incorporated into α_{i3}C20/(min·mol of enzyme). *Insets*: Lineweaver–Burk transformation of the data; no plot using simple weighting could be drawn for the C180 peptide. Transformation of the data with the Hill equation was required to obtain the $S_{0.5}$ and k_{cat} values reported in Table 2. $S_{0.5} = (K')^{1/n}$, where n = the Hill coefficient and K' is a constant comprising the interaction factors and the intrinsic dissociation constant (Segel, 1975).

between the two substrates. The catalytic efficiency ($k_{cat}/K_{m\alpha_{i3}C20}$ or $k_{cat}/S_{0.5\alpha_{i3}C20}$) was 0.16 for C180, 0.07 for C204, and 0.05 for rS1 (Table 2). Although we must consider that an inhibitor, present in the α_{i3}C20 peptide preparations, could contribute to the observed kinetic activities of the C180 peptide, the fact that neither the C204 peptide nor S1 peptide showed the same kinetic profile as C180 argues against this possibility.

These data indicated that C180 possessed similar affinities for both NAD and α_{i3}C20 and a similar k_{cat} for the ADP-ribosylation of α_{i3}C20 as S1. This showed that the amino-terminal 180 amino acids of S1 comprise the entire ADP-ribosyltransferase mechanism and the NAD and α_{i3}C20 binding sites. These data also showed that although the 55 carboxyl-terminal residues of S1 did not include residues that directly participated in the ADP-ribosylation of α_{i3}C20, the C204 deletion peptide possessed a linear velocity profile that was intermediate to C180 and S1 at variable α_{i3}C20. This suggested that the carboxyl-terminal region of S1 was required to maintain the functional independence of the NAD and α_{i3}C20 binding sites.

Table 3: ADP-ribosylation of the Heterotrimeric, G_t, and α_{i3}C20 by C180 or rS1

peptide	target	velocity[a] [mol/(min·mol)]	ratio G_t/α_{i3}C20
C180	G_t	0.07 ± 0.01	1.4
	α_{i3}C20	0.04 ± 0.01	
rS1	G_t	0.85 ± 0.07	28
	α_{i3}C20	0.03 ± 0.01	

[a] Incubations were as described in Materials and Methods with 10 μM NAD and 0.5 μM of either α_{i3}C20 or G_t. Values are the average of two separate experiments performed at 4 °C.

rS1- and C180-Catalyzed ADP-ribosylation of α_{i3}C20 and G_t. C180 catalyzed the ADP-ribosylation of G_t and α_{i3}C20 at similar rates (less than 2-fold difference), while rS1 catalyzed the ADP-ribosylation of G_t at a 28-fold higher rate than α_{i3}C20 (Table 3). Earlier studies showed that C180 ADP-ribosylated G_t at about 1% of the efficiency of rS1, that rS1 possessed a lower K_{mGt} and higher k_{cat} than C180 in the ADP-ribosylation reaction, and that a carboxyl-terminal deletion peptide of S1 that was composed of the amino-terminal 204 amino acids of S1 possessed similar ADP-ribosylation activity as S1 (Cortina *et al.*, 1991; Krueger & Barbieri, 1994). Together, these data imply the presence of two separate G protein binding sites within S1. One G protein binding site is located within the amino-terminal 180 amino acids of S1 and is represented by the binding of α_{i3}-C20 to C180. Two models are envisioned for the organization of the second G protein binding site that is defined by residues 195–204 of S1 and is responsible for the high affinity binding of G_t to S1. In the first model, residues 195–204 of S1 interact directly with a region of $G_{t\alpha}$ that is distinct from α_{i3}C20 and is defined by the heterotrimeric conformation of G_t. In the second model, rather than representing a second G protein binding site, residues 195–204 modify an amino-terminal region of S1 into a high affinity G protein binding site. In the second model, since S1 and C180 possess similar affinities for α_{i3}C20, the second G protein binding site within the amino-terminal region of S1 would occur outside the α_{i3}C20 binding site. This second G protein binding site of S1 appears to interact with $G_{t\alpha}$ rather than $G_{t\beta\gamma}$, since Birnbaumer and co-workers (Graf *et al.*, 1992) observed that $G_{t\beta\gamma}$ did not stimulate the ADP-ribosylation of α_{i3}C20 by PT (Table 3). Thus, $G_{t\beta\gamma}$ does not appear to interact directly with S1.

Integration of the crystal structure of pertussis toxin (Stein *et al.*, 1994) with the kinetic analysis performed in the present study allows several predictions about the structure–function properties of S1. First, the crystal structure of PT was consistent with residues 195–204 of S1 participating in the ADP-ribosylation reaction as a binding site for $G_{t\alpha}$ since these residues were located adjacent to the proposed active site

within S1. Second, the crystal structure of pertussis toxin was consistent with the two G protein binding sites within S1 being located in discontinuous regions of S1 rather than residues 195−204 representing a continuum of the α_{i3}C20 binding site. In the crystal structure residues 153−190 of S1, which separate the active site where α_{i3}C20 presumably binds from residues 195 to 204, are located on the exterior surface of S1 and do not appear to contribute directly to the organization of the active site.

ACKNOWLEDGMENT

α_{i3}C20 was synthesized at the Shared Protein-Nucleic Acid Research Facility at MCW under the supervision of Liane M. Mende-Mueller.

REFERENCES

Barbieri, J. T., Rappuoli, R., & Collier, R. J. (1987) *Infect. Immun. 55*, 1321−1323.

Barbieri, J. T., Moloney, B. K., & Mende-Mueller, L. M. (1989) *J. Bacteriol. 171*, 4362−4369.

Barbieri, J. T., Pizza, M., Cortina, G., & Rappuoli, R. (1990) *Infect. Immun. 58*, 999−1003.

Birnbaumer, L., Abramowitz, J., & Brown, A. M. (1990) *Biochim. Biophys. Acta 1031*, 163−224.

Burnette, W. N., Mar, V. L., Cieplak, W., Morris, K. T., Kaljot, K. S., Marchitto, R. K., Sachdev, C., Locht, C., & Keith, J. M. (1988) *Bio/Technology 6*, 699−706.

Conklin, B. R., & Bourne, H. R. (1993) *Cell 73*, 631−641.

Cortina, G., & Barbieri, J. T. (1991) *J. Biol. Chem. 266*, 3022−3030.

Cortina, G., Krueger, K. M., & Barbieri, J. T. (1991) *J. Biol. Chem. 266*, 23810−23814.

Graf, R., Codina, J., & Birnbaumer L. (1992) *Mol. Pharmacol. 42*, 760−764.

Hsia, J. A., Tsai, S., Adamik R., Yost D. A., Hewlett, E. L., & Moss, J. (1985) *J. Biol. Chem. 260*, 16187−16191.

Katada, T., Tamura, M., & Ui, M. (1983) *Arch. Biochem. Biophys. 224*, 290−298.

Krueger, K. M., & Barbieri, J. T. (1993) *J. Biol. Chem. 268*, 12570−12578.

Krueger, K. M., & Barbieri, J. T. (1994) *Infect. Immun. 61*, 307−313.

Locht, C., & Keith, J. M. (1986) *Science 232*, 1258−1264.

Locht, C., Cieplak, W., Marchitto, K. S., Sato, H., & Keith, J. H. (1987) *Infect. Immun. 55*, 2546−2553.

Locht, C., Lobet, Y., Feron, C., Cieplak, W., & Keith, J. M. (1990) *J. Biol. Chem. 265*, 4552−4559.

Nicosia, A., Perugini, M., Franzini, C., Casagli, M. C., Borri, M. G., Antoni, G., Almoni, M., Neri, P., Ratti, G., & Rappuoli R. (1986) *Proc. Natl. Acad. Sci. U.S.A. 83*, 4631−4635.

Nicosia, A., Bartolini, A., Perugini, M., & Rappuoli, R. (1987) *Infect. Immun. 55*, 963−967.

Segel, I. H. (1975) in *Enzyme kinetics*, Wiley, New York, NY.

Stein, P. E., Boodhoo, A., Armstrong, G. D., Cockle, S. A., Klein, M. H., & Read, R. J. (1994) *Structure 2*, 45−57.

Tamura, M., Nogimori, K., Murai, M., Yajima, M., Ito, K., Katada, T., Ui, M., & Ishii, S. (1982) *Biochemistry 21*, 5516−5522.

Ui, M. (1990) in *ADP-ribosylating toxins and G proteins; insights into signal transduction* (Moss, J., & Vaughan, M., Eds) pp 45−66, American Society for Microbiology, Washington, DC.

Van Dop, C., Yamanaka, G., Steinberg, F., Sekura, R., D., Manclark, C. R., Stryer, L., & Bourne, H. (1984) *J. Biol. Chem. 259*, 23−26.

Watkins, P. A., Burns, D. L., Kanaho, Y., Liu, T., Hewlett, E. L., & Moss, J. (1985) *J. Biol. Chem. 260*, 13478−13482.

Weiss, A. A., & Falkow, S. (1984) *Infect. Immun. 43*, 263−269.

West, R. E., Jr., Moss, J., Vaughan, M., Liu, T., & Liu T. (1985) *J. Biol. Chem. 260*, 14428−14430.

Xu, Y., Barbançon-Finck, V., & Barbieri, J. T. (1994) *J. Biol. Chem. 269*, 1−7.

BI9405306